1 Unstable periodic discrete minimal surfaces

Konrad Polthier

Technische Universität Berlin, Institut für Mathematik
polthier@math.tu-berlin.de

Summary. In this paper we define the new *alignment energy* for non-conforming triangle meshes, and describes its use to compute unstable conforming discrete minimal surfaces. Our algorithm makes use of the duality between conforming and non-conforming discrete minimal surfaces which was observed earlier. In first experiments the new algorithm allows us the computation of unstable periodic discrete minimal surfaces of high numerical precision. The extraordinary precision of the discrete mesh enables us to compute the index of several triply periodic minimal surfaces.

1.1 Introduction

The numerical computation of unstable discrete minimal surfaces with *excellent numerical qualities* is among the most challenging problems. Good quality means that the numerical solution is sufficiently accurate to allow further investigations of the numerical data set. For example, discrete minimal surfaces are critical points of the discrete area functional and the calculation of the second derivative of the area functional at such a critical point requires that the discrete mesh is of very high numerical quality, i.e. very close to an exact critical point. Away from a critical point the second derivative is of minor value. Currently, good data sets of unstable discrete minimal surfaces are very hard to produce, even worse, they are hardly available to the community. Solutions obtained by integrating the Weierstrass functions are usually interpolating the smooth surface very well at the vertices but have unknown variational properties and are usually not discrete minimal surfaces in our sense.

In this paper we introduce a new algorithm to compute solutions of free-boundary value problems of minimal surfaces where the boundaries are constrained to meet a collection of planes orthogonally, or equivalently, to consist of planar symmetry lines lying on a set of given planes. For example, a patch may be bounded by the faces of a convex polyhedron like the images in Figures 1.7 and 1.8. To circumvent the instability of solutions of free boundary value problems one can use an indirect approach when the conjugate minimal surface is stable - this is the so-called conjugate surface construction [3][4]. It is known from our previous work [7][8] that all discrete minimal surfaces come in pairs of a *conforming* and a conjugate *non-conforming* surface. Non-conforming triangle meshes are characterized by the property that

adjacent triangles are connected at their edge midpoints rather than having both endpoints of the edge in common.

In order to compute a conforming discrete minimal surface via the conjugate surface construction one computes its non-conforming conjugate minimale surface. But non-conforming meshes are highly unstable with respect to the area functional, such that, previous to this work, non-conforming minimal surfaces could only be obtained by starting from a conforming discrete minimal surface.

The essential ingredient in our algorithm is the introduction of the new *alignment energy* for non-conforming triangle meshes. It turns out that minimizing the alignment energy in the class of *non-conforming* triangle meshes leads to non-conforming discrete minimal surfaces whose discrete conjugate surfaces are then solutions of free-boundary value problems for *conforming* triangle meshes.

In a previous work [9] we computed unstable conforming discrete catenoids and helicoids by deriving explicit formulas for the vertices. Brakke's surface evolver [1] allows usage of the Hessian to reach an unstable critical point if the surface is already near enough the critical point for the Hessian mode to work.

This paper first introduces in Section 1.2 the different types of discrete minimal surfaces relevant for our discussion, and recalls in Section 1.3 the duality of conforming and non-conforming discrete minimal surfaces. In Section 1.4 we introduce the new alignment energy for non-conforming discrete minimal surfaces which is the basis on a new algorithm for unstable conforming minimal surfaces. We conclude with a number of test computations of well-known triply periodic minimal surfaces, and a numerical evaluation of their index.

1.2 Review of Non-Conforming Triangle Meshes

In the theory of discrete minimal surfaces we observed the simultaneous appearance of two different types of triangle meshes, so-called conforming and non-conforming triangle meshes [7][8]. Because of their importance for the present work we recall their definitions.

Definition 1. *A* simplicial surface M_h *in* $\mathbb{R}^m$ *is a simplicial complex consisting of a finite set* $\mathfrak{T}$ *of planar triangles such that*

1. *Any vertex* $p \in M_h$ *belongs to at least one triangle* $T \in \mathfrak{T}$.
2. *The star of each vertex* $p \in M_h$ *is a simplicial disk.*

Note, a simplicial surface is continuous across edges and at the vertices of its triangles. We follow the common practice in finite element theory to call a simplicial surface a *conforming surface*.

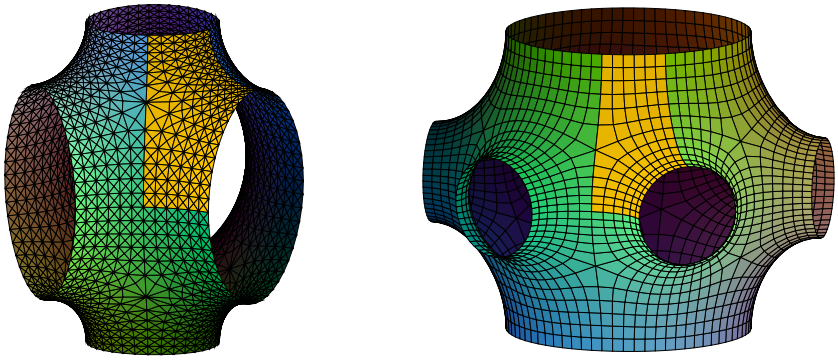

Fig. 1.1. Discrete H-T surface with fundamental patch in a 3-prism, and differently assembled in a 6-prism. In the right figure sets of four coplanar triangles were joined to emphasize the observed alignment of edges with curvature lines.

Definition 2. *On a simplicial surface M_h we define the function space S_h of* conforming functions*:*

$$S_h := \left\{ v : M_h \to \mathbb{R}^d \;\middle|\; v \in C^0(M_h) \text{ and } v \text{ is linear on each triangle} \right\}$$

S_h is a finite dimensional space spanned by the Lagrange basis functions $\{\varphi_1, .., \varphi_n\}$ corresponding to the set of vertices $\{p_1, ..., p_n\}$ of M_h, that is for each vertex p_i we have a function

$$\begin{gathered} \varphi_i : M_h \to \mathbb{R} \\ \varphi_i(p_j) = \delta_{ij} \quad \forall i, j \in \{1, .., n\} \\ \varphi_i \text{ is linear on each triangle.} \end{gathered} \tag{1.1}$$

Then each function $u_h \in S_h$ has a unique representation

$$u_h(p) = \sum_{j=1}^{n} u_j \varphi_j(p) \quad \forall\, p \in M_h$$

where $u_j = u_h(p_j) \in \mathbb{R}^d$.

Second, we introduce the following space of non-conforming finite elements. Since this space includes discontinuous functions its use was sometimes called a *variational crime* in the finite element literature [2]. In our setting of discrete minimal surfaces the space of non-conforming functions and surfaces does naturally appear [7][8].

Definition 3. *For a simplicial surface M_h, we define the space of* non-conforming functions *by*

$$S_h^* := \left\{ v : M_h \to \mathbb{R}^d \;\middle|\; \begin{array}{l} v_{|T} \text{ is linear for each } T \in M_h, \text{ and} \\ v \text{ is continuous at all edge midpoints} \end{array} \right\}.$$

The space S_h^* is a superset of the space of conforming functions S_h, since S_h^* additionally includes functions which are discontinuous at edges away from the edge midpoint. Let $\{m_i\}$ denote the set of edge midpoints of M_h, then for each midpoint m_i we have the basis function

$$\begin{gathered} \psi_i : M_h \to \mathbb{R} \\ \psi_i(m_j) = \delta_{ij} \quad \forall\, i,j \in \{1,2,..\} \\ \psi_i \text{ is linear on each triangle.} \end{gathered} \tag{1.2}$$

Note, that ψ_i may be multi-valued along edges. The support of a function ψ_i consists of the (at most two) triangles adjacent to the edge e_i, and ψ_i is usually not continuous on M_h. Each function $v \in S_h^*$ has a representation

$$v_h(p) = \sum_{\text{edges } e_i} v_i \psi_i(p) \quad \forall\, p \in M_h$$

where $v_i = v_h(m_i)$ is the value of v_h at the edge midpoint m_i of e_i.

We will use the term *non-conforming surface* M_h^* to denote the image of a simplicial surface under a non-conforming function.

1.3 Discrete Minimal Surfaces

The area of a conforming or non-conforming simplicial surface is defined as the sum of the area of all elements. This leads to the following variational characterization of discrete minimal surfaces which applies both to conforming and non-conforming meshes:

Definition 4. *A conforming surface M_h respectively non-conforming surface M_h^* is a* discrete minimal surface *iff the discrete area functional of M_h respectively M_h^* is critical with respect to variations of any set of interior vertices respectively interior edge midpoints. To include symmetry properties into this definition we allow a constrained variation of boundary points:*

- *if a boundary segment is a straight line, then its points may vary along the straight line*
- *if a boundary segment is a planar curve, then its points may vary within the plane*
- *in all other cases the boundary points always remain fixed.*

The relaxed boundary constraints allow one to solve free boundary value problems such that a discrete minimal surfaces may be extended by reflection to a discrete minimal surface. We recall the explicit representation of the area gradient given in [6]:

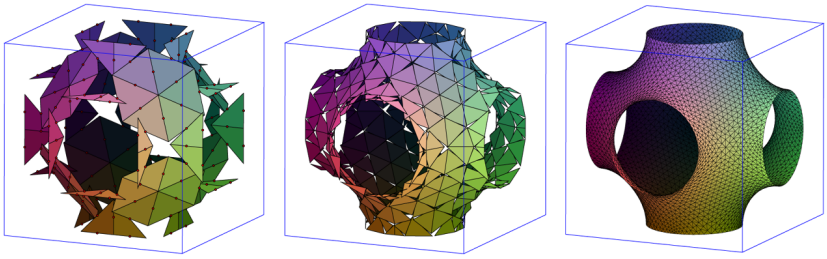

Fig. 1.2. Free-boundary value problem of Schwarz P-surface in a cube solved via the discrete conjugate surface construction of [6]. The solution of that method is a non-conforming discrete minimal surface which is shown here at different discretizations.

Lemma 1. *A simplicial surface M_h is discrete minimal if and only if at each interior vertex p*

$$\frac{d}{dp}\operatorname{area} M_h = \frac{1}{2}\sum_j (\cot\alpha_j + \cot\beta_j)(p - q_j) = 0 \tag{1.3}$$

where $\{q_j\}$ denotes the set of vertices of link p *and α_j,β_j denote the two angles opposite to the edge pq_j. At boundary vertices on symmetry arcs the area gradient is constrained to be tangential to the straight line or to the plane.*

For non-conforming surfaces we have the following representation of the area functional which was derived in [7]:

Lemma 2. *A non-conforming surface M_h^* is discrete minimal if it solves a system of equations such that at each edge midpoint m_i we have*

$$\begin{aligned}\frac{d}{dm_i}\operatorname{area} M_h^* &= 2(\cot\alpha_{i_{-2}}\cdot(m_i - m_{i_{-1}}) + \cot\alpha_{i_{-1}}\cdot(m_i - m_{i_{-2}}) \\ &\quad + \cot\alpha_{i_1}\cdot(m_i - m_{i_2}) + \cot\alpha_{i_2}\cdot(m_i - m_{i_1})) \\ &= 0.\end{aligned} \tag{1.4}$$

where $\{i_{-2}, i_{-1}, i_1, i_2,\}$ denote subindices of adjacent edge midpoints m_i as shown in Figure 1.3 (assuming that v is the identity map in the figure, i.e. angles are measure in M_h^*).

Note, this theorem is true for the larger class of non-conforming Laplace-Beltrami harmonic maps v on a simplicial surface where the area gradient generalizes to the gradient of the Dirichlet energy, see [7].

1.3.1 Duality of Conjugate Discrete Minimal Surfaces

The following theorem obtained in [7] justifies the two definitions of discrete minimal surfaces. It states the general relation between conjugate pairs of discrete minimal surfaces.

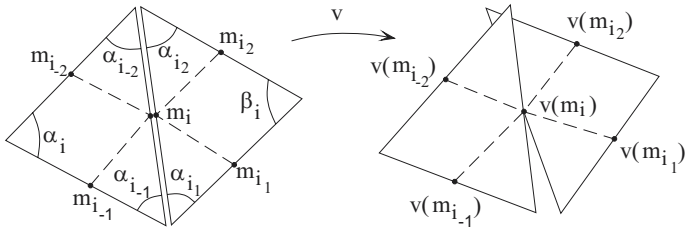

Fig. 1.3. A non-conforming map is given by its value on edge midpoints.

Theorem 1. *Let N be a simplicial surface in $\mathbb{R}^m$ and let S_h respectively S_h^* be the space of conforming respectively non-conforming immersions of N into $\mathbb{R}^d$. Then*

1. Let $M_h \subset \mathbb{R}^d$ be a discrete minimal surface in S_h. Then there exists a conjugate surface $M_h^* \subset \mathbb{R}^d$ in S_h^* which is critical for the area functional in S_h^*.

2. Let $M_h \subset \mathbb{R}^d$ be a discrete minimal surface in S_h^*. Then there exists a conjugate surface $M_h^* \subset \mathbb{R}^d$ in S_h which is critical for the area functional in S_h.

3. M_h^* is uniquely determined by M_h up to translation.

4. M_h and M_h^* are isometric and have the same Gauss map in the sense that corresponding triangles are congruent and parallel.

5. Applying the conjugation twice leads to

$$M_h^{**} = -M_h$$

for a suitably chosen origin.

Summarizing, the theorem shows that a pair of conjugate discrete minimal surfaces generically does not exist in the space of piecewise linear conforming elements S_h but naturally leads to the space of piecewise linear non-conforming Crouzeix-Raviart elements S_h^* [2]. S_h alone is too rigid to contain the conjugate of a minimal surface.

At first sight, this theorem seems to suggest a strategy for solving free-boundary problems for conforming meshes, namely, to simulate the *conjugate surface construction* which worked so well for smooth minimal surfaces [3][4]. That means, assume a given free boundary value problem for a conforming mesh, then solve the conjugate Dirichlet problem with a non-conforming mesh. The conjugate of the non-conforming minimal surface is then a conforming solution of the original problem.

The problem with this strategy is that the area functional for non-conforming meshes is not stable. Consider two adjacent triangles which are coplanar and whose corresponding edges enclose a positive angle. Then Figure 1.4 indicates that the joint area of both triangles may be reduced by moving

the common edge midpoint towards the intersection of the lines through the other edge midpoints. This movement continuously reduces the common area to zero while not affecting any other parts of the surfaces. In practice this degeneration of pairwise triangles is the default behaviour when minimizing the area functional of non-conforming meshes.

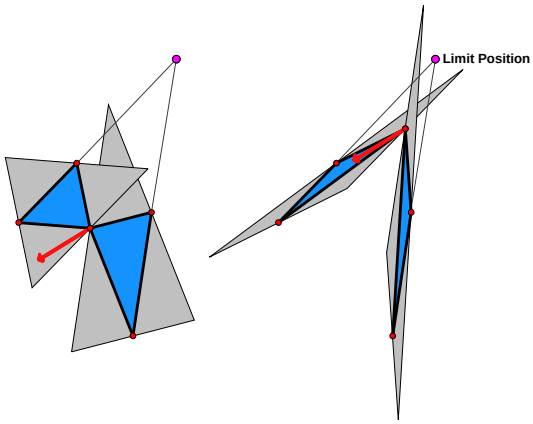

Fig. 1.4. This example shows the instability of the area functional for non-conforming meshes. Two adjacent coplanar triangles with non-parallel edge degenerate to two triangles with zero area.

1.4 The Alignment Energy

The stability of the area functional of conforming simplicial surfaces is often spoiled by tangential motion of vertices which leads to degenerate triangles. As noted in [6] degenerate triangles may often be removed in practical implementations but in general there is no strategy available which tells existence of a discrete solution of a boundary value problem when assuming a given underlying mesh connectivity.

The situation with non-conforming meshes is even worse since basically there do not exist stable minimizers, i.e. discrete minimizers which are stable under small pertubations of their vertices.

Therefore, we will experiment with the following new energy for non-conforming surfaces which promises to be much more stable. This energy is designed to minimize the gradient of the non-conforming area functional instead of the functional itself.

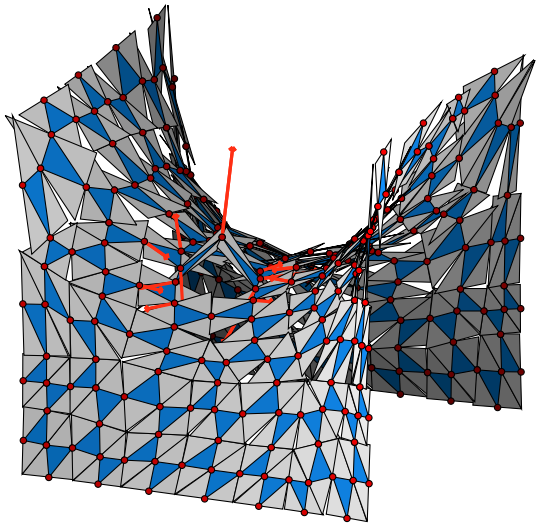

Fig. 1.5. Non-conforming mesh with a stencil of a vertex for the alignment energy and the induced gradients. The marked vertex has been moved away from its equilibrium position.

Note, minimizing the gradient instead of the functional is a common practice, for example, if the numerical accuracy is to be improved.

We begin with the following definition of a rotation operator on a simplicial surface.

Definition 5. *Assume that the boundary of each triangle of a conforming or non-conforming surface is oriented. Two adjacent triangles may have different orientations, which means, we include non-orientable surfaces. Then the* rotation operator *J is defined as a rotation by $\frac{\pi}{2}$ within the plane of each triangle such that for each edge c the vector Jc is orthogonal to c and points into the interior of the triangle.*

Consider a pair of adjacent triangles T_1 and T_2 whose edges c_1 and c_2 are connected at their midpoint.

Definition 6. *The* alignment energy *of a non-conforming surface M_h^* is given by*

$$E(M_h^*) := \sum_{edge\ c \in \mathring{M}} |J_1 c_1 + J_2 c_2|^2 + \frac{1}{2} \sum_{edge\ c \in \partial M} |Jc + Rot_c Jc|^2 \qquad (1.5)$$

where c_1 and c_2 represent the edge c in each of the two adjacent triangles T_1 and T_2 of c. At a boundary edge c the comparison vector $Rot_c Jc$ is produced by rotating Jc around c by π

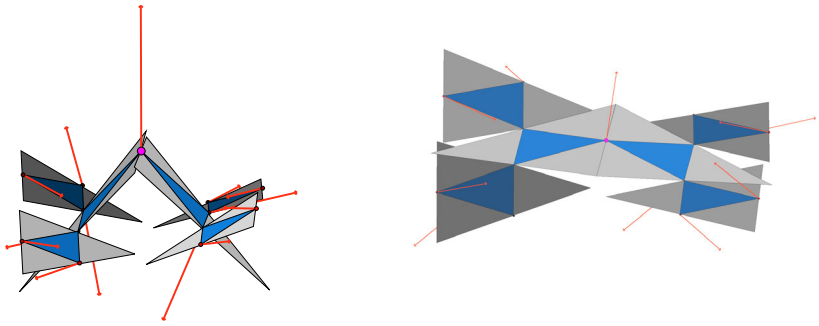

Fig. 1.6. Stencil of the alignment energy associated to an edge midpoint. Each vertex contributes to the alignment energy of the six triangles of its 2-star.

The alignment energy measures two entities simultaneously: first, the angle between the two corresponding midperpendiculars at an edge, and second, the difference in length of c_1 and c_2. That means, the alignment energy $|J_1c_1 + J_2c_2|^2$ of an edge is zero if c_1 and c_2 have equal lengths and if the two corresponding midperpendiculars are parallel, i.e. both triangles are *aligned* at the common edge midpoint m.

For computational purposes we calculate the gradient of the alignment energy. The edge midpoint m of c contributes to all edges of T_1 and T_2.

$$\frac{d}{dm}E(M) = \frac{d}{dm}\begin{pmatrix} |J_1c_1 + J_2c_2|^2 \\ +|J_{1,1}a_{1,1} + J_1a_1|^2 + |J_{1,2}b_{1,2} + J_1b_1|^2 \\ +|J_{2,1}a_{2,1} + J_2a_2|^2 + |J_{2,2}b_{2,2} + J_2b_2|^2 \end{pmatrix} \tag{1.6}$$

In a non-conforming triangle (m, q, r), where m, q, r are midpoints of the edges $c = -2c_m, a = -2a_m, b = -2b_m$ and where a_m, b_m, c_m are the edges of the mid-quarter triangle, we have

$$\begin{aligned} \nabla_m Jc &= (\cot\alpha + \cot\beta)NN^t \\ \nabla_m Ja &= +J\circ\pi - \cot\beta NN^t \\ \nabla_m Jb &= -J\circ\pi - \cot\alpha NN^t. \end{aligned} \tag{1.7}$$

The contribution of each triangle T_1 to the gradient of the alignment energy at m is

$$\begin{aligned} \frac{d}{dm}E(M)^t = 2((&\cot\alpha_1 + \cot\beta_1)\, N_1N_1^t \cdot J_2c_2 \\ &+ (\cot\alpha_2 + \cot\beta_2)\, N_2N_2^t \cdot J_1c_1 \\ &+a_1 + \left(-J_1 - \cot\beta_1 N_1N_1^t\right) \cdot J_{1,1}a_{1,1} \\ &-b_1 + \left(+J_1 - \cot\alpha_1 N_1N_1^t\right) \cdot J_{1,2}b_{1,2}). \end{aligned} \tag{1.8}$$

The importance of the alignment energy is a consequence of the following observation.

Theorem 2. *Let M_h^* be a non-conforming surface. Then M_h^* is a discrete minimal surface if and only if M_h^* has vanishing alignment energy.*

Proof. Let T be a triangle with oriented edges $a = b + c$, and angles α and β opposite to a and b. Then we have

$$-Jc = \cot\alpha \cdot a + \cot\beta \cdot b.$$

The assumption is now an immediate consequence of theorem 1.4 and equation 1.4 since we can write the area gradient of M_h^* as

$$\frac{d}{dm_i}\text{area}\, M_h^* = J_1 c_1 + J_2 c_2.$$

Since the alignment energy vanishes exactly if it vanishes at every edge, a minimizer of the alignment energy is a non-conforming discrete minimal surface, and vice versa.

As a corollary of the preceeding lemma we obtain from theorem 1 that the discrete conjugation provides the following 1-1 pairing:

Corollary 1. *There exists a duality between non-conforming minimizers of the alignment energy and conforming discrete minimal surface.*

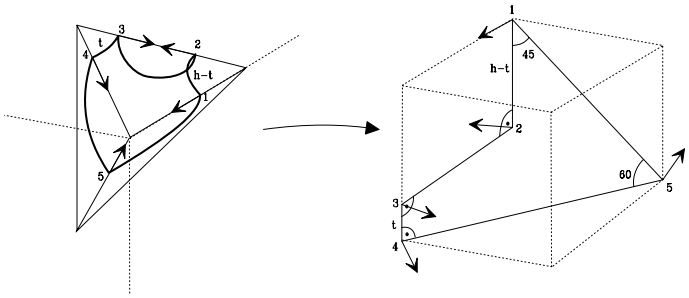

Fig. 1.7. Transformation of a free-boundary value problem into a family of Dirichlet boundary value problems.

1.4.1 Algorithm for Free-Boundary Value Problems

Corollary 1 suggests the following algorithm to compute solutions of free-boundary value problems for minimal surfaces. The method is similar to the algorithms in [6] for solving free-boundary value problems for minimal surfaces and in [5] for computing discrete constant mean curvature surfaces in $\mathbb{R}^3$ by minimizing surface area in $\mathbb{S}^3$. In contrast to our method, both

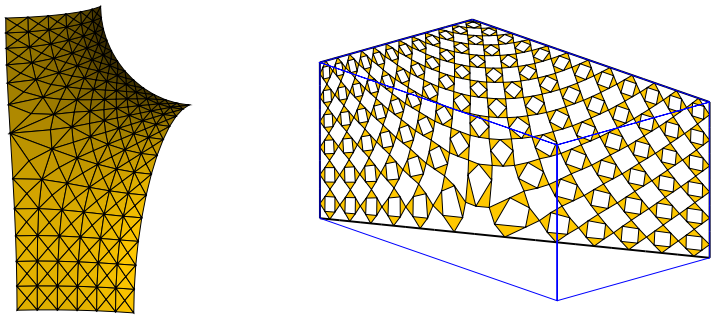

Fig. 1.8. Pair of conjugate fundamental patches of the H-T surface. The non-conforming mesh on the right was obtained by minimizing the alignment energy, and then conjugated to the conforming surface on the left (the right figure shows the mid-quarter of each triangle).

previous methods obtained non-conforming solutions of the free-boundary value problem while we obtain conforming solutions. Following the remark on the stability of the area functional of non-conforming surfaces, conforming solutions are much better suited, for example, to compute the index of discrete minimal surfaces.

The following algorithm assumes a background knowledge of the conjugate surface construction of smooth minimal surfaces to obtain the conjugate contour Γ consisting of straight lines from a given free-boundary contour consisting of a collection of planes [4]. Note, in general the lengths of $n-4$ edges of Γ are unknown parameters (when ignoring scaling), which means, one must consider a family of contours Γ if there are more than 4 boundary segments.

Alignment Algorithm Given a free-boundary value problem for a minimal surface, and assuming the conjugate contour Γ is known.

1. Solve the Dirichlet problem in Γ for the alignment energy among non-conforming surfaces. Denote the minimizer M_h^*.
2. Compute the conjugate conforming surface from M_h^*. The conjugate M_h is a conforming discrete minimal surface.

The first step produces a non-conforming discrete minimal surface. The second step of the algorithm is the same as the conjugation operation of discrete harmonic maps introduced in [6] except that it is applied here to non-conforming meshes. For discrete minimal surfaces the conjugation operation amounts to rotating each triangle by $\frac{\pi}{2}$ in the plane of each triangle and then assembling the triangles at corresponding edges. Note, theorem 1 ensures that this operation leads to a conforming discrete minimal surface.

1.4.2 Comparison of Stability Properties

We consider a contour consisting of segments of straight lines, as in Figure 1.9, which typically appears in boundary value problems for periodic minimal surfaces. In practice we assume that the boundary vertices may freely move along their boundary segment in order to allow extension of a solution by reflection at the boundary segments, see Definition 4. For a given initial triangulation one observes that minimizing the area functional often leads to degenerate situations where triangles shrink to an edge. This instability of the discrete area functional is well-known and is related to tangential motions of the vertices. The same effect occurs when iteratively minimizing the Dirichlet energy, although each step is more stable. See [6] which justifies the removal of degenerate triangles.

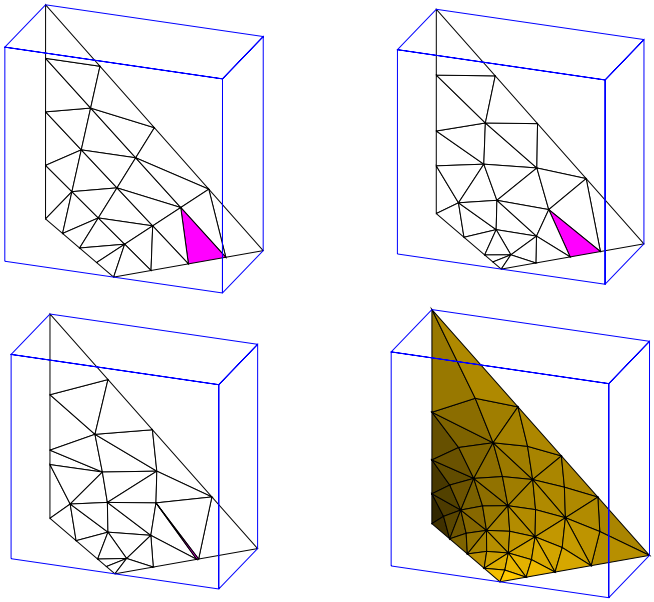

Fig. 1.9. Minimizing the area functional may lead to degenerate triangulations even for simple boundary contours. Although the Dirichlet energy is more stable its iterative minimization leads to the same degeneracies. In the sequence of three figures a triangle shrinks to an edge. The fourth figure at the bottom right uses an apropriate triangulation to avoid degeneration.

When considering the degeneracy phenomenon from a combinatorial point of view then one can say that an immersion as a discrete minimal surface does not exist for every given combinatorial mesh. An example for the non-existence of immersions is easily constructed as shown in Figure 1.10 where it is obvious that the two free boundary points must move to a degenerate

situation. The set of combinatorial meshes, which may be realized as discrete minimal surfaces in a given boundary contour, cannot be estimated yet but it seems that the number of realizable combinatorial meshes for a given boundary value problem may be quite restricted.

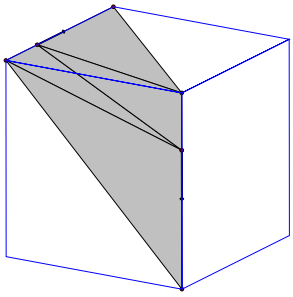

Fig. 1.10. Non-existence of a minimal immersion of a combinatorial mesh in a given boundary value problem. The two points will finally move to vertices of the contour as indicated by their area gradients.

The situation in the non-conforming case is even worse. Basically, every non-conforming discrete minimal surface is unstable for the discrete area functional. A small pertubation of two adjacent triangles of a non-conforming discrete minimal surface may lead to a degenerate situation as indicated in Figure 1.4 for two coplanar triangles. If the common edge is not parallel then the common midpoint of this edge may be moved to the intersection of the two lines spanned by the other two edge midpoints in each triangle. It is easily seen that the area of the two quarter triangles, which is always a quarter of the full triangle, decreases to zero.

The described instability makes the area functional useless for computing non-conforming minimal surfaces. This is the place where the alignment energy appears. As demonstrated in this paper the alignment energy seems to be reasonably stable and an efficient tool for computing unstable discrete minimal surfaces.

1.5 Examples of Discrete Triply Periodic Minimal Surfaces

We now report on some experiments we performed with triply periodic minimal surfaces. A detailed background on the minimal surfaces are given in [3][4]. Different previous approaches for the computation of these surfaces have been done. The first known computation by Anderson used the fact that the fundamental patch for the symmetry group of certain surfaces solves a

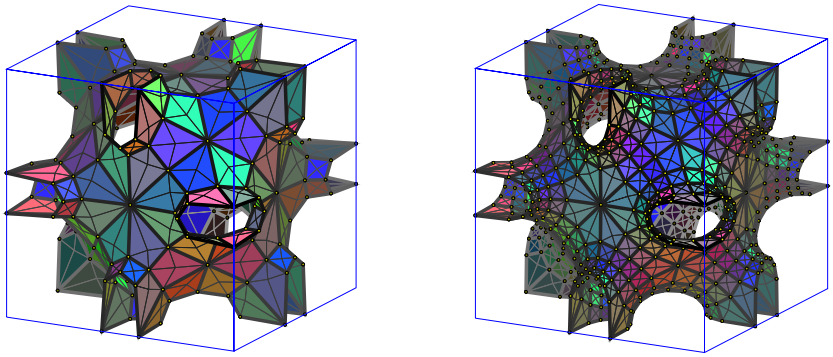

Fig. 1.11. Discrete versions of Neovius surface in a cube. Note the observation that in both minimizers each triangle has three coplanar adjacent triangles which leads to a tessellation with planar quadrilaterals.

free-boundary value in a tetrahedron and that the patch is a graph in tetrahedral coordinates. Pinkall and Polthier [6] introduced the conjugation of discrete conforming minimal surfaces which leads to non-conforming meshes as shown in Figure 1.2. This method was later extended to compute constant mean curvature surfaces by Oberknapp and Polthier [5] through discrete minimal surfaces in $\mathbb{S}^3$. Both methods used an adhoc approach to produce a conforming mesh from the obtained non-conforming surface since non-conforming meshes were not considered as valid mathematical objects during those days. Note, the averaging step can be justified to produce good results as indicated in Figure 1.2. Brakke has successfully computed several triply periodic minimal surfaces by specifying volume constraints [1] and by minimizing a discrete Willmore energy which is the integral of mean curvature squared.

The following experiments were produced with the algorithm 1.4.1 and aim at directly producing conforming discrete minimal surfaces.

The eigenvalue computations follow the discrete setup of Polthier and Rossman [9]. Note, for the experiments described in that paper more complicated unstable discrete minimal surfaces were not available yet. The discrete surfaces produced via minimizing the alignment energy turn out to have a sufficient numerical accuracy.

1.5.1 Index of F-Rd

A building block of the F-Rd surface is bounded by a cube as shown in Figure 1.12. The discrete minimal surface has a very small area gradient. As a consequence we obtain basically no tangential eigenfunctions, that means, the numerically computed index 9 is rather accurate. We plan to submit the datasets of this surface and the following I-Wp surface to the EG-Models

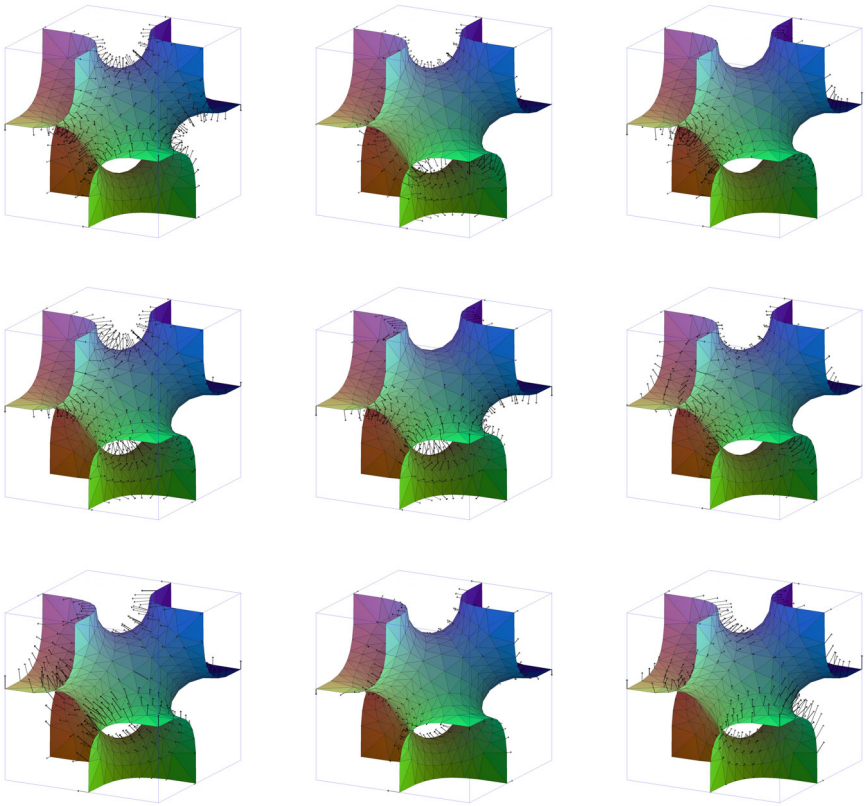

Fig. 1.12. Numerically found 9 eigenfunctions of the discrete F-Rd surface with negative eigenvalues.

server at www.eg-models.de to enable comparison of our results with other numerical algorithms.

Vertices/Elements 430/768
Area/Gradient 15.006517086292167/0.000000000053007
9 negative and first zero eigenvalues of the discrete F-Rd surface.

eValue[0] = -0.1504559679908802	eValue[5] = -0.03865424556938688
eValue[1] = -0.09904128162525966	eValue[6] = -0.004015601274444393
eValue[2] = -0.09904128162524234	eValue[7] = -0.004015601274391426
eValue[3] = -0.09904128162524005	eValue[8] = -0.004015601274380579
eValue[4] = -0.03865424556948896	eValue[9] = -2.7290174465353138E-28

1.5.2 Index of I-Wp

We computed the index of the I-Wp surface at different solutions. It turned out that already the very coarsest resolution gave the same answer 19 for the

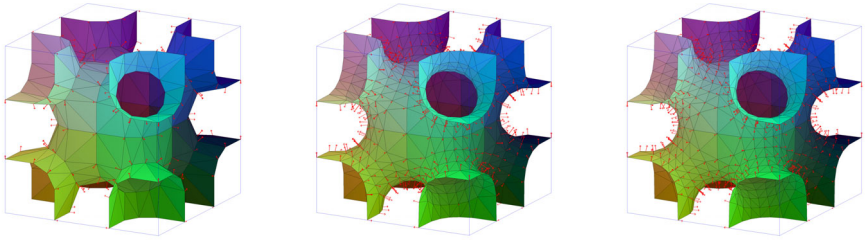

Fig. 1.13. I-Wp surface at different resolutions with first eigenvector.

number of negative eigenvalues. The finer resolutions confirmed this result but did not have the same small gradient but only of the order of 1.E-6. This larger numerical error led to a few tangential eigenfunctions with small negative eigenvalues but which were clearly distinguishable from the normal eigenfunctions.

Vertices/Elements 234/384
Area/Gradient 40.187264207966614/0.000000000006771
19 negative and first zero eigenvalues of the discrete I-Wp surface.

eValue[0] = -0.632087803765472	eValue[10] = -0.13011897222983074
eValue[1] = -0.5175825952322985	eValue[11] = -0.13011897222982016
eValue[2] = -0.5175825952322736	eValue[12] = -0.1301189722297763
eValue[3] = -0.5175825952322616	eValue[13] = -0.05465367417861271
eValue[4] = -0.37793138360297224	eValue[14] = -0.054653674157824385
eValue[5] = -0.3779313836029666	eValue[15] = -0.054653674137100865
eValue[6] = -0.37793138360293166	eValue[16] = -0.04551152809511838
eValue[7] = -0.2598562604031981	eValue[17] = -0.04551152809511528
eValue[8] = -0.2249510919234355	eValue[18] = -0.045511528095097585
eValue[9] = -0.22495109192343474	eValue[19] = -8.039329159488626E-28

References

1. K. A. Brakke. The surface evolver. *Exp. Math.*, 1(2):141–165, 1992.
2. S. C. Brenner and L. R. Scott. *The Mathematical Theory of Finite Element Methods*. Springer Verlag, 1994.
3. H. Karcher. The triply periodic minimal surfaces of A. Schoen and their constant mean curvature compagnions. *Man. Math.*, 64:291–357, 1989.
4. H. Karcher and K. Polthier. Construction of triply periodic minimal surfaces. In J. Klinowski and A. L. Mackay, editors, *Curved Surfaces in Chemical Structures*, volume 354 (1715) of *A*, pages 2077–2104. The Royal Society, London, Great Britain, phil. trans. r. soc. lond. edition, September 1996.
5. B. Oberknapp and K. Polthier. An algorithm for discrete constant mean curvature surfaces. In H.-C. Hege and K. Polthier, editors, *Visualization and Mathematics*, pages 141–161. Springer Verlag, Heidelberg, 1997.

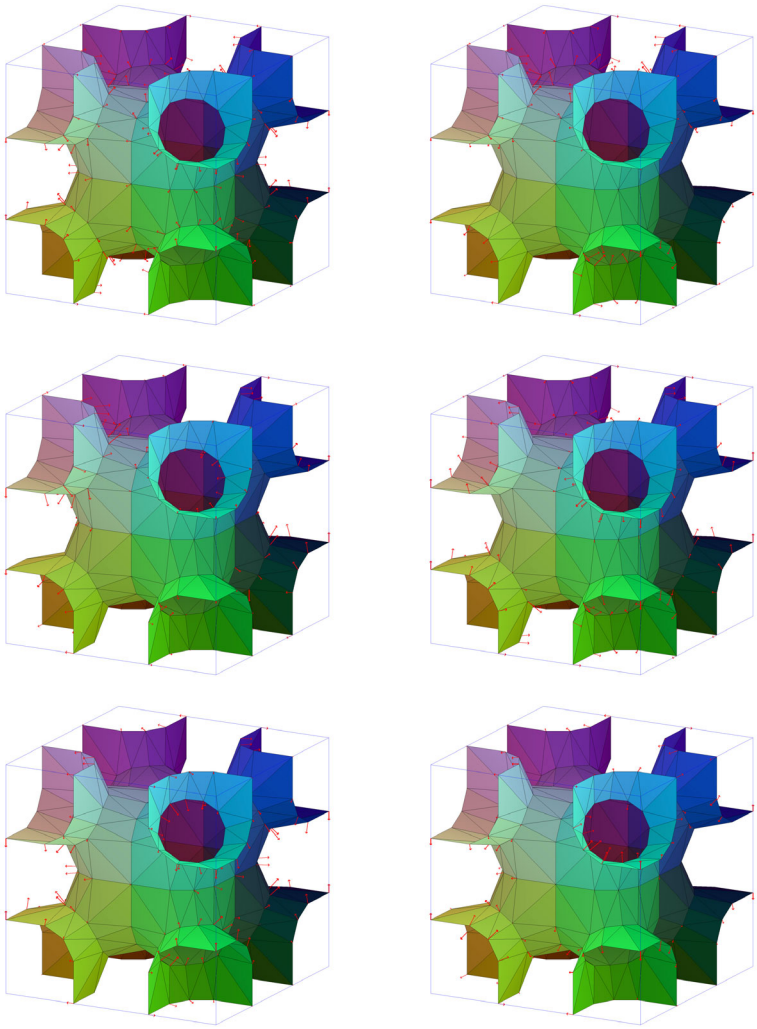

Fig. 1.14. First six (0,1,4,7,8,10) of the numerically found 19 eigenfunctions of the discrete I-Wp surface with negative eigenvalues.

6. U. Pinkall and K. Polthier. Computing discrete minimal surfaces and their conjugates. *Experim. Math.*, 2(1):15–36, 1993.
7. K. Polthier. Conjugate harmonic maps and minimal surfaces. Report 446, SFB 288, TU-Berlin, 2000.
8. K. Polthier. Computational aspects and discrete minimal surfaces. In D. Hoffman, editor, *Proc. of the Clay Summerschool on Minimal Surfaces*. AMS, 2002.
9. K. Polthier and W. Rossman. Discrete constant mean curvature surfaces and their index. *J. reine angew. Math*, 549(47–77), 2002.